THE SECOND-ORDER GRAVITATIONAL REDSHIFT

– TRACKING ANALYSIS STUDY –

Grant NGR 09-015-205

Final Report

Principal Investigators

Jack Jaffe and Robert F. C. Vessot

October 1973

Prepared for

National Aeronautics and Space Administration
Marshall Space Flight Center
Alabama 35812

Smithsonian Institution
Astrophysical Observatory
Cambridge, Massachusetts 02138

THE SECOND-ORDER GRAVITATIONAL REDSHIFT

– TRACKING ANALYSIS STUDY –

Grant NGR 09-015-205

Final Report

Principal Investigators

Jack Jaffe and Robert F. C. Vessot

October 1973

Prepared for

National Aeronautics and Space Administration
Marshall Space Flight Center
Alabama 35812

Smithsonian Institution
Astrophysical Observatory
Cambridge, Massachusetts 02138

ABSTRACT

A first-phase, perturbation analysis is presented for the tracking requirements necessary for the measurement of the second-order redshift in a heliocentric probe experiment. The clock performance required for such an experiment is also investigated.

THE SECOND-ORDER GRAVITATION REDSHIFT

– TRACKING ANALYSIS STUDY –

Jack Jaffe and Robert F. C. Vessot

Center for Astrophysics
Harvard College Observatory and Smithsonian Astrophysical Observatory
Cambridge, Massachusetts 02138

1. INTRODUCTION

The second-order redshift experiment is one of two tests that is currently feasible of the second-order term in the theories of gravitation. To date, the only second-order test is the measurement of the perihelion advance of a planet or space probe; all the other current experimental tests of relativity measure first-order effects only.

A second-order redshift experiment basically consists of sending a space probe containing a very stable atomic clock as close to the sun as possible and comparing its frequency with an identical clock on earth by use of light or microwave signals. If the gravitational potential difference is sufficiently great, compared to the relative stability of the two clocks, the second-order term should be measurable. An analysis of the basic theory and equations of this experiment, as well as model orbit calculations, have been completed in an earlier phase of this study (Jaffe and Vessot, 1973).

It is worth noting that one advantage of an experiment of this kind is that "idealized" orbits, which would necessitate "drag-free" probe tolerances, are not required.

This paper is basically concerned with a first-phase analysis of the actual tracking requirements necessary for measuring the second-order redshift. This analysis has then been applied to various model orbits of heliocentric probes, such as the proposed NASA–ESRO heliocentric satellite mission.

This work was supported in part by grant NGR 09-015-205 from the National Aeronautics and Space Administration.

2. SECOND-ORDER GRAVITATIONAL REDSHIFT

We can establish the maximum requirements for the necessary accuracy of the tracking parameters by application of the perturbation technique. The determination of the minimum allowable requirements would necessitate a more extensive analysis, by using the correlation and covariance matrix approach. This is beyond the present scope of this phase of the study and would be the next logical step in a more detailed study of the redshift experiment.

We will first establish the tracking-accuracy requirements for the parameters as they are originally written in the heliocentric coordinate system. These accuracy requirements will then be converted into the earth-based coordinate system.

For an earth-based observer, the "doppler-canceled" redshifted signal z received at the earth station from the probe is, in heliocentric coordinates (Jaffe and Vessot, 1973),

$$
\begin{aligned}
z = \frac{\Delta\nu}{\nu} = {} & \left[\left(\frac{m}{r_1} - \frac{m}{r_2}\right) + \frac{1}{2}\left(\beta_1^2 - \beta_2^2\right)\right] + A_e\left(A'_p - A_e\right) \\
& - \left(A'_p - A_e\right)\left[\left(\frac{m}{r_1} - \frac{m}{r_2}\right) + \frac{1}{2}\left(\beta_1^2 - \beta_2^2\right) + A_e\left(A'_p - A_e\right)\right] \\
& + m\left[\gamma\left(\frac{\beta_{r_1}^2}{r_1} - \frac{\beta_{r_2}^2}{r_2}\right) + \frac{3}{2}\frac{\beta_1^2}{r_1} - \frac{1}{2}\frac{\beta_2^2}{r_2} - \frac{1}{2}\left(\frac{\beta_2^2}{r_1} + \frac{\beta_1^2}{r_2}\right)\right] \\
& + \frac{1}{8}\left(3\beta_1^4 - \beta_2^4 - 2\beta_1^2\beta_2^2\right) + m^2\left[(\beta - \gamma)\left(\frac{1}{r_2^2} - \frac{1}{r_1^2}\right) + \frac{3}{2}\frac{1}{r_1^2} - \frac{1}{2}\frac{1}{r_2^2} - \frac{1}{r_1}\frac{1}{r_2}\right] \\
& + \left(A'_p - A_e\right)\left\{A'_p\left[\left(\frac{m}{r_1} - \frac{m}{r_2}\right) + \frac{1}{2}\left(\beta_1^2 - \beta_2^2\right) + A_e\left(A'_p - A_e\right)\right] + A_e^3\right\} ,
\end{aligned}
\tag{1}
$$

where $m \equiv GM/c^2$, $\beta_i \equiv v_i/c$ (G and c are set = 1 throughout), $\beta_i^2 = \beta_{r_i}^2 + r^2\beta_{\theta_i}^2$, $A_e \equiv \vec{\beta}_1 \cdot \vec{\epsilon}_{12}$, and $A'_p \equiv \vec{\beta}_2 \cdot \vec{\epsilon}_{12}$, in which $\vec{\epsilon}_{ij} = [\sqrt{A/B}\ \sqrt{1 - (B\ell^2/r^2)},\ \ell/r,\ 0]$ is the generalized "direction vector" of the light signal from position i to position j; ℓ is a constant of the motion for the light signal, $B \equiv 1 - (2m/r) + (\beta - \gamma)\ (2m^2/r^2)$, and $A \equiv 1 + \gamma\,(2m/r)$. The unsubscripted parameters, β and γ, are the so-called Eddington-Robertson coefficients (Jaffe and Vessot, 1973).

3. DETERMINATION OF ℓ IN TERMS OF THE BOUNDARY CONDITIONS

Before proceeding with the specific perturbation analysis, we must first determine ℓ in terms of r_1, θ_1, r_2, and θ_2. This can be done by using the geodesic equations of motion for light. We first carry out the calculation in the absence of gravity, and then we repeat this analysis for the spherically symmetric gravitational field.

In the absence of gravity, all the $g_{ij} = 1$, and the relevant geodesic equations for light in the (r, θ, ϕ, t) coordinate system are as follows (Jaffe, 1969):

$$r^2 \frac{d\theta}{ds} = \text{constant} \equiv p \quad ,$$

$$\frac{dt}{ds} = \text{constant} \equiv q \quad ,$$

$$\frac{p}{q} = \text{constant} \equiv \ell \quad ;$$

ℓ can be interpreted as the impact parameter as measured at infinity. The ϕ equation is not necessary here, for light can be confined to motion on a plane; this is true both in the classical and in the general relativistic cases.

For $g_{ij} = 1$, the metric is simply

$$ds^2 = dt^2 - dr^2 - r^2 \, d\theta^2 \quad .$$

For the case of light, $ds^2 = 0$.

Combining these equations, we have

$$\left(\frac{dr}{d\theta}\right)^2 = \frac{r^4}{\ell^2} - r^2 \quad ,$$

$$\int d\theta = \pm \int \frac{\ell \, dr}{r\sqrt{r^2 - \ell^2}} \quad .$$

The $\pm$ sign depends on the direction of the light signal. This equation can be integrated to yield

$$\theta = \pm \cos^{-1} \left(\frac{\ell}{r}\right) + \theta_0 \quad ,$$

where θ_0 is the point at which $\left.\frac{dr}{d\theta}\right|_{\theta=\theta_0} = 0$. The corresponding value of r, the so-called turning point, is defined as d_0, i.e., $\left.\frac{dr}{d\theta}\right|_{r=d_0} = 0$.

We have

$$\theta_1 = - \cos^{-1} \left(\frac{\ell}{r_1}\right) + \theta_0 \quad ,$$

$$\theta_2 = \cos^{-1} \left(\frac{\ell}{r_2}\right) + \theta_0 \quad .$$

Subtracting the second equation from the first and taking the cosine of both sides yield

$$\cos (\theta_2 - \theta_1) = \frac{1}{r_1 r_2} [\ell^2 - (r_1^2 - \ell^2)^{1/2} (r_2^2 - \ell^2)^{1/2}] \quad .$$

By solving for ℓ, we finally have

$$\ell = \frac{r_1 r_2 \sin (\theta_2 - \theta_1)}{\sqrt{r_1^2 + r_2^2 - 2r_1 r_2 \cos (\theta_2 - \theta_1)}} \quad . \qquad (2)$$

Since, classically, light moves in a straight line, the "impact parameter at infinity," ℓ, is indeed the value of the distance of closest approach at the point of closest approach. Thus,

$$\ell \equiv d_0 \quad .$$

This is not the case in general relativity, as will be seen below.

We now repeat the calculations in the general relativistic framework. We will use the exact Schwarzschild field here, instead of the Eddington-Robertson expansion, for the spherically symmetric gravitational field, because it is somewhat simpler to manipulate and is quite sufficient for our present purposes. The Schwarzschild field is given as

$$ds^2 = A\, dt^2 - \frac{dr^2}{A} - r^2\, d\theta^2 \quad ,$$

where $A \equiv 1 - 2m/r$. For light, $ds^2 = 0$.

The relevant geodesic equations are

$$r^2 \frac{d\theta}{ds} = \text{constant} \equiv p \quad ,$$

$$A \frac{dt}{ds} = \text{constant} \equiv q \quad ,$$

$$\frac{p}{q} = \ell \quad ,$$

where ℓ can again be interpreted as the impact parameter as measured at infinity. Combining these equations gives

$$\left(\frac{dr}{d\theta}\right)^2 = \frac{r^4}{\ell^2} - A\, r^2 \quad ; \tag{3}$$

$\frac{dr}{d\theta} = 0$ at $r = d$. This yields

$$\ell^2 = \frac{d^2}{A} = \frac{d^2}{1 - (2m/d)}$$

or

$$\ell = \frac{d}{\sqrt{1 - (2m/d)}} \quad . \tag{4}$$

Thus, ℓ does not have the same value as the turning point, d. By integrating equation (3), we have

$$\int d\theta = \pm \int \frac{\ell \, dr}{r\sqrt{r^2 - A\ell^2}}$$

$$\underset{d>>m}{\approx} d^{3/2} \int \frac{dr}{r^{1/2}\sqrt{r^3 d - d^3 r - 2m(r^3 - d^3)}}$$

$$= d \int \frac{dr}{r\sqrt{r^2 - d^2}} \left[1 + \frac{m}{d} + \frac{md}{r(r+d)}\right]$$

$$= \cos^{-1}\frac{d}{r} + \frac{m}{d}\sqrt{r^2 - d^2}\left[\frac{2r + d}{r(r+d)}\right] + \theta_0 \quad , \tag{5}$$

where θ_0 is the value of θ where $\left.\frac{dr}{d\theta}\right|_{\theta=\theta_0} = 0$.

Accordingly,

$$\theta_0 - \theta_1 = \cos^{-1}\frac{d}{r_1} + \frac{m}{d}\sqrt{r_1^2 - d^2}\left[\frac{2r_1 + d}{r_1(r_1 + d)}\right] \quad ,$$

$$\theta_2 - \theta_0 = \cos^{-1}\frac{d}{r_2} + \frac{m}{d}\sqrt{r_2^2 - d^2}\left[\frac{2r_2 + d}{r_2(r_2 + d)}\right] \quad .$$

Adding these two equations and taking the cosine of both sides yield

$$\cos\left(\cos^{-1}\frac{d}{r_2}+\cos^{-1}\frac{d}{r_1}\right)=\frac{1}{r_1r_2}\left(d^2-\sqrt{r_2^2-d^2}\,\sqrt{r_1^2-d^2}\right)$$

$$\approx\cos(\theta_2-\theta_1)+\frac{m}{d_0}\left[\sqrt{r_2^2-d_0^2}\,\frac{2r_2+d_0}{r_2(r_2+d_0)}\right.$$

$$\left.+\sqrt{r_1^2-d_0^2}\,\frac{2r_1+d_0}{r_1(r_1+d_0)}\right]\sin(\theta_2-\theta_1)\quad.$$

Solving for d, we obtain

$$d=\frac{r_2r_1\left\{1-\left[\cos(\theta_2-\theta_1)+(m/d_0)\,E\sin(\theta_2-\theta_1)\right]^2\right\}^{1/2}}{\left\{r_1^2+r_2^2-2r_1r_2\left[\cos(\theta_2-\theta_1)+(m/d_0)\,E\sin(\theta_2-\theta_1)\right]\right\}^{1/2}}$$

$$\approx\frac{r_2r_1\sin(\theta_2-\theta_1)}{\sqrt{r_1^2+r_2^2-2r_1r_2\cos(\theta_2-\theta_1)}}\left\{1-\frac{m}{d_0}\,E\left[\operatorname{ctn}(\theta_2-\theta_1)\right.\right.$$

$$\left.\left.-\frac{r_1r_2\sin(\theta_2-\theta_1)}{r_1^2+r_2^2-2r_1r_2\cos(\theta_2-\theta_1)}\right]\right\}\quad,\qquad(6)$$

where

$$E=\sqrt{r_2^2-d_0^2}\,\frac{2r_2+d_0}{r_2(r_2+d_0)}+\sqrt{r_1^2-d_0^2}\,\frac{2r_1+d_0}{r_1(r_1+d_0)}\quad.$$

Comparing equation (6) with equation (2), we see that

$$d = d_0 \left\{ 1 + \frac{m}{d_0} E \left[\frac{d_0}{\sqrt{r_1^2 + r_2^2 - 2r_1 r_2 \cos(\theta_2 - \theta_1)}} - \operatorname{ctn}(\theta_2 - \theta_1) \right] \right\} . \tag{7}$$

By use of equation (4), ℓ can finally be written as

$$\ell \approx d \left(1 + \frac{m}{d}\right) \approx d_0 \left\{ 1 + \frac{m}{d_0} + \frac{m}{d_0} E \left[\frac{d_0}{\sqrt{r_1^2 + r_2^2 - 2r_1 r_2 \cos(\theta_2 - \theta_1)}} - \operatorname{ctn}(\theta_2 - \theta_1) \right] \right\} . \tag{8}$$

4. PERTURBATION ANALYSIS IN THE HELIOCENTRIC SYSTEM

We will first carry out a perturbation analysis with respect to the heliocentric space-probe parameters r_2, θ_2, v_{r_2}, v_{θ_2}. Errors due to uncertainties in the earth-based observer's parameters (r_1, θ_1, ...) will be significantly smaller, and need not be considered here in an analysis of the most stringent tracking accuracies required.

4.1 Radial Velocity

Differentiating equation (1) with respect to β_{r_2}, we have

$$\Delta z = \left(- \beta_{r_2} + A_e \sqrt{1 - \frac{\ell^2}{r_2^2}} \right) \Delta\beta_{r_2} \quad . \tag{9}$$

Lower order terms in v/c need not be retained here, since we are solving for the maximum uncertainty in the parameter that will still allow detection of the second-order (in m/r = fourth order in v/c) redshift effect.

4.2 Angular Velocity

Differentiating equation (1) with respect to β_{θ_2}, we have

$$\Delta z = (- r_2^2 \beta_{\theta_2} + A_e \ell) \Delta\beta_{\theta_2} \quad . \tag{10}$$

4.3 Radial Distance

We differentiate equation (1) with respect to r_2. This result is more involved than the preceding equations, since ℓ is also a function of r_2 and θ_2. We find

$$\Delta z = \frac{m}{r_2}\,\frac{\Delta r_2}{r_2} - r_2\,\beta_{\theta_2}^2\,\Delta r_2 + A_e\left[\frac{\beta_{r_2}}{\sqrt{1-(\ell^2/r_2^2)}}\,\frac{\ell^2}{r_2^2}\,\frac{1}{r_2}\right.$$

$$\left. + \left(\frac{-\beta_{r_2}}{\sqrt{1-(\ell^2/r_2^2)}}\,\frac{\ell}{r_2}\,\frac{1}{r_2} + \beta_{\theta_2}\right)\frac{\partial \ell}{\partial r_2}\right]\Delta r_2$$

$$+ (A_p' - 2A_e)\left[\frac{-\beta_{r_1}}{\sqrt{1-(\ell^2/r_1^2)}}\,\frac{\ell}{r_1}\,\frac{1}{r_1} + \beta_{\theta_1}\,\Delta r_2\right]\frac{\partial \ell}{\partial r_2}\,\Delta r_2 \quad , \tag{11}$$

where

$$\ell = \frac{r_1 r_2 \sin(\theta_2 - \theta_1)}{\sqrt{r_1^2 + r_2^2 - 2r_1 r_2 \cos(\theta_2 - \theta_1)}} \quad . \tag{12}$$

(The corrections in m/d to ℓ need not be retained here, for the same reasons as given above.) And,

$$\frac{\partial \ell}{\partial r_2} = \frac{r_1^2 \sin(\theta_2 - \theta_1)[r_1 - r_2 \cos(\theta_2 - \theta_1)]}{[r_1^2 + r_2^2 - 2r_1 r_2 \cos(\theta_2 - \theta_1)]^{3/2}} \quad . \tag{13}$$

4.4 Angle

Differentiating equation (1) with respect to θ_2 yields

$$\Delta z = A_e\left[\frac{-\beta_{r_2}}{\sqrt{1-(\ell^2/r_2^2)}}\,\frac{\ell}{r_2^2} + \beta_{\theta_2}\right]\frac{\partial \ell}{\partial \theta_2}\,\Delta\theta_2$$

$$+ (A_p' - 2A_e)\left[\frac{-\beta_{r_1}}{\sqrt{1-(\ell^2/r_1^2)}}\,\frac{\ell}{r_1^2} + \beta_{\theta_1}\right]\frac{\partial \ell}{\partial \theta_2}\,\Delta\theta_2 \quad , \tag{14}$$

where

$$\frac{\partial \ell}{\partial \theta_2} = \frac{r_1 r_2 \cos(\theta_2 - \theta_1)[r_1^2 + r_2^2 - r_1 r_2 \cos(\theta_2 - \theta_1)] - r_1^2 r_2^2}{[r_1^2 + r_2^2 - 2r_1 r_2 \cos(\theta_2 - \theta_1)]^{3/2}} \quad . \tag{15}$$

5. CONVERSION FROM HELIOCENTRIC SYSTEM TO GEOCENTRIC SYSTEM

It is sufficient at this stage of the analysis to make a plane-geometry conversion from the sun-centered coordinate system to the earth-centered system. From Figure 1, we have

$$\vec{r} = \vec{R} + \vec{\rho} \quad ,$$

$$r^2 = R^2 + \rho^2 + 2\vec{R} \cdot \vec{\rho}$$

and

$$\dot{\vec{r}} = \dot{\vec{R}} + \dot{\vec{\rho}} \quad ,$$

$$\beta^2 \underset{c=1}{\equiv} \dot{r}^2 = \dot{R}^2 + \dot{\rho}^2 + 2\dot{\vec{R}} \cdot \dot{\vec{\rho}} \quad .$$

The unit vectors in the r and θ directions can be written as

$$\hat{e}_r = \cos\theta\,\hat{i} + \sin\theta\,\hat{j}$$

$$= \sqrt{1 - \sin^2\theta}\,\hat{i} + \sin\theta\,\hat{j} \quad ,$$

$$\hat{e}_\theta = -\sin\theta\,\hat{i} + \cos\theta\,\hat{j}$$

$$= -\sin\theta\,\hat{i} + \sqrt{1 - \sin^2\theta}\,\hat{j} \quad ,$$

where $\hat{i}$ and $\hat{j}$ are the unit vectors in the x and y directions (in the heliocentric system). By the law of sines,

$$\frac{\sin\theta}{\rho} = \frac{\sin\phi}{r} \quad , \tag{16}$$

or

$$\sin\theta = \frac{\rho}{r}\sin\phi \quad .$$

We finally have

$$\hat{e}_r = \sqrt{1 - \frac{\rho^2}{r^2}\sin^2\phi}\,\hat{i} + \frac{\rho}{r}\sin\phi\,\hat{j} \quad ,$$

with

$$r^2 = R^2 + \rho^2 - 2R\rho\cos\phi \quad ,$$

an expression for $\hat{e}_r$ written solely in terms of the earth-based coordinates ρ, ϕ, and R. Similarly,

$$\hat{e}_\theta = -\frac{\rho}{r}\sin\phi\,\hat{i} + \sqrt{1 - \frac{\rho^2}{r^2}\sin^2\phi}\,\hat{j} \quad .$$

We can now write β_r and β_θ completely in terms of the earth-based coordinates:

$$\beta_r = \vec{\beta}\cdot\hat{e}_r = (\vec{\dot{R}} + \vec{\dot{\rho}})\cdot\hat{e}_r \quad ,$$

where $\vec{\dot{\rho}}$ has the components

$$\vec{\dot{\rho}} = \dot{\rho}\,\hat{\rho} + \rho\,\dot{\phi}\,\hat{\phi}$$

$$= -(\rho\sin\phi\,\dot{\phi} + \dot{\rho}\cos\phi)\,\hat{i} + (\rho\cos\phi\,\dot{\phi} - \dot{\rho}\sin\phi)\,\hat{j} \quad .$$

The earth's motion, $\vec{\dot{R}}$, is assumed here to be uniform and circular; i.e.,

$$\vec{\dot{R}} = -R\,\omega\sin\omega t\,\hat{i} + R\,\omega\cos\omega t\,\hat{j} \quad .$$

Corrections to this assumption will be discussed in a later section.

We finally obtain

$$\beta_r = (\dot{\vec{R}} + \dot{\vec{\rho}}) \cdot \hat{e}_r$$

$$= - (R\,\omega \sin \omega t + \rho \sin\phi\,\dot{\phi} + \dot{\rho}\cos\phi) \sqrt{1 - \frac{\rho^2}{r^2}\sin^2\phi}$$

$$+ (R\,\omega \cos \omega t + \rho \cos\phi\,\dot{\phi} - \dot{\rho}\sin\phi)\frac{\rho}{r}\sin\phi \quad , \tag{17}$$

with

$$r^2 = R^2 + \rho^2 - 2R\rho\cos\phi \quad . \tag{18}$$

Similarly,

$$r\beta_\theta = (\dot{\vec{R}} + \dot{\vec{\rho}}) \cdot \hat{e}_\theta$$

$$= (R\,\omega \sin \omega t + \rho \sin\phi\,\dot{\phi} + \dot{\rho}\cos\phi)\frac{\rho}{r}\sin\phi$$

$$+ (R\,\omega \cos \omega t + \rho \cos\phi\,\dot{\phi} - \dot{\rho}\sin\phi)\sqrt{1 - \frac{\rho^2}{r^2}\sin^2\phi} \quad . \tag{19}$$

6. PERTURBATION ANALYSIS IN THE GEOCENTRIC SYSTEM

The preceding section has established the functional relationships of the parameters in the heliocentric system with respect to those in the geocentric system. We must now consider the resultant uncertainty in these geocentric parameters that is associated with the allowable uncertainty in the heliocentric parameters.

$\underline{r_2}$:

From equation (18),

$$r_2 = (R^2 + \rho^2 - 2R\rho \cos \phi)^{1/2} \quad .$$

Therefore,

$$\Delta r_2 = \frac{\partial r_2}{\partial R} \Delta R + \frac{\partial r_2}{\partial \rho} \Delta \rho + \frac{\partial r_2}{\partial \phi} \Delta \phi$$

$$= \frac{R - \rho \cos \phi}{(R^2 + \rho^2 - 2R\rho \cos \phi)^{1/2}} \Delta R \qquad (20a)$$

$$+ \frac{\rho - R \cos \phi}{(R^2 + \rho^2 - 2R\rho \cos \phi)^{1/2}} \Delta \rho \qquad (20b)$$

$$+ \frac{R \rho \sin \phi}{(R^2 + \rho^2 - 2R\rho \cos \phi)^{1/2}} \Delta \phi \quad . \qquad (20c)$$

$\underline{\theta_2}$:

From equation (16),

$$\theta_2 = \sin^{-1} \left(\frac{\rho}{r_2} \sin \phi \right) \quad .$$

Therefore,

$$\Delta\theta_2 = \frac{\partial\theta_2}{\partial R}\Delta R + \frac{\partial\theta_2}{\partial\rho}\Delta\rho + \frac{\partial\theta_2}{\partial\phi}\Delta\phi$$

$$= -\frac{R - \rho\cos\phi}{[1 - (\rho^2/r_2^2)\sin^2\phi]^{1/2}} \frac{\rho\sin\phi}{r_2^3}\Delta R \tag{21a}$$

$$+ \frac{1}{[1 - (\rho^2/r_2^2)\sin^2\phi]^{1/2}} \left[\frac{\sin\phi}{r_2} - \frac{\rho\sin\phi}{r_2^3}(\rho - R\cos\phi)\right]\Delta\rho \tag{21b}$$

$$+ \frac{1}{[1 - (\rho^2/r_2^2)\sin^2\phi]^{1/2}} \left[\frac{\rho\cos\phi}{r_2} - \frac{\rho\sin\phi}{r_2^3}(R\rho\sin\phi)\right]\Delta\phi \quad . \tag{21c}$$

β_{r_2} :

From equation (17),

$$\Delta\beta_{r_2} = \frac{\partial\beta_{r_2}}{\partial\rho}\Delta\rho + \frac{\partial\beta_{r_2}}{\partial\dot{\rho}}\Delta\dot{\rho} + \frac{\partial\beta_{r_2}}{\partial\phi}\Delta\phi + \frac{\partial\beta_{r_2}}{\partial\dot{\phi}}\Delta\dot{\phi} + \frac{\partial\beta_{r_2}}{\partial R}\Delta R + \frac{\partial\beta_{r_2}}{\partial\omega}\Delta\omega$$

$$= \Bigg\{ - \sin\phi\,\dot{\phi}\sqrt{1 - \frac{\rho^2}{r_2^2}\sin^2\phi} - (R\,\omega\sin\omega t + \rho\sin\phi\,\dot{\phi} + \dot{\rho}\cos\phi)$$

$$\times \left(1 - \frac{\rho^2}{r_2^2}\sin^2\phi\right)^{-1/2}\left[-\frac{\rho\sin^2\phi}{r_2^2} + \frac{\rho^2\sin^2\phi}{r_2^4}(\rho - R\cos\phi)\right]$$

$$+ \cos\phi\,\dot{\phi}\frac{\rho}{r_2}\sin\phi + (R\,\omega\cos\omega t + \rho\cos\phi\,\dot{\phi} - \dot{\rho}\sin\phi)$$

$$\times \left[\frac{\sin\phi}{r} - \frac{\rho\sin\phi}{r_2^3}(\rho - R\cos\phi)\right]\Bigg\}\Delta\rho \tag{22a}$$

$$- \left(\cos\phi \sqrt{1 - \frac{\rho^2}{r_2^2} \sin^2\phi} + \sin^2\phi \frac{\rho}{r_2} \right) \Delta\dot{\rho} \qquad (22b)$$

$$+ \left[- (\rho \cos\phi \dot{\phi} - \dot{\rho} \sin\phi) \sqrt{1 - \frac{\rho^2}{r_2^2} \sin^2\phi} - (R \omega \sin \omega t + \rho \sin\phi \dot{\phi} + \dot{\rho} \cos\phi) \right.$$

$$\times \left(- \frac{2\rho^2 \sin\phi \cos\phi}{r_2^2} + \frac{2\rho^3 \sin^2\phi R}{r_2^4} \right) - (\rho \sin\phi \dot{\phi} + \dot{\rho} \cos\phi) \frac{\rho}{r^2} \sin\phi$$

$$+ (R \omega \cos \omega t + \rho \cos\phi \dot{\phi} - \dot{\rho} \sin\phi)$$

$$\left. \times \left(\frac{\rho \cos\phi}{r_2} - \frac{\rho \sin\phi}{r_2^3} R \rho \sin\phi \right) \right] \Delta\phi \qquad (22c)$$

$$- \left(\rho \sin\phi \sqrt{1 - \frac{\rho^2}{r_2^2} \sin^2\phi} - \rho \cos\phi \frac{\rho}{r_2} \sin\phi \right) \Delta\dot{\phi} \qquad (22d)$$

$$- \left[\omega \sin \omega t \sqrt{1 - \frac{\rho^2}{r_2^2} \sin^2\phi} \right.$$

$$\left. + (R \omega \sin \omega t + \rho \sin\phi \dot{\phi} + \dot{\rho} \cos\phi) \left(1 - \frac{\rho^2}{r_2^2} \sin^2\phi \right)^{-1/2} \right.$$

$$\left. \times \frac{\rho^2 \sin^2\phi}{r_2^4} (R - \rho \cos\phi) - \omega \cos \omega t \frac{\rho}{r_2} \sin\phi \right.$$

$$\left. + (R \omega \cos \omega t + \rho \cos\phi \dot{\phi} - \dot{\rho} \sin\phi) \frac{\rho \sin\phi}{r_2^3} (R - \rho \cos\phi) \right] \Delta R \qquad (22e)$$

$$- \left[(R \sin \omega t + \omega^2 R \cos \omega t) \sqrt{1 - \frac{\rho^2}{r_2^2} \sin^2 \phi} \right.$$

$$\left. + (R \cos \omega t - \omega^2 R \sin \omega t) \frac{\rho}{r} \sin \phi \right] \Delta\omega \quad . \tag{22f}$$

$\underline{\beta_{\theta_2}}$:

From equation (19),

$$\Delta\beta_{\theta_2} = \frac{\partial\beta_{\theta_2}}{\partial\rho} \Delta\rho + \frac{\partial\beta_{\theta_2}}{\partial\dot{\rho}} \Delta\dot{\rho} + \frac{\partial\beta_{\theta_2}}{\partial\phi} \Delta\phi + \frac{\partial\beta_{\theta_2}}{\partial\dot{\phi}} \Delta\dot{\phi} + \frac{\partial\beta_{\theta_2}}{\partial R} \Delta R + \frac{\partial\beta_{\theta_2}}{\partial\omega} \Delta\omega$$

$$= \frac{1}{r_2} \left\{ \sin\phi \, \dot{\phi} \frac{\rho}{r_2} \sin\phi + (R\,\omega \sin\omega t + \rho \sin\phi \, \dot{\phi} + \dot{\rho} \cos\phi) \right.$$

$$\times \left[\frac{\sin\phi}{r_2} - \frac{\rho \sin\phi}{r_2^3} (\rho - R\cos\phi) \right] + \cos\phi \, \dot{\phi} \sqrt{1 - \frac{\rho^2}{r_2^2} \sin^2\phi}$$

$$+ (R\,\omega \cos\omega t + \rho \cos\phi \, \dot{\phi} - \dot{\rho} \sin\phi) \left[- \frac{\rho \sin^2\phi}{r_2^2} + \frac{\rho^2 \sin^2\phi}{r_2^4} (\rho - R\cos\phi) \right]$$

$$- \frac{1}{r_2} \left[(R\,\omega \sin\omega t + \rho \sin\phi \, \dot{\phi} + \dot{\rho} \cos\phi) \frac{\rho}{r_2} \sin\phi \right.$$

$$\left. + (R\,\omega \cos\omega t + \rho \cos\phi \, \dot{\phi} - \dot{\rho} \sin\phi) \sqrt{1 - \frac{\rho^2}{r_2} \sin^2\phi} \right]$$

$$\left. \times \frac{\rho - R\cos\phi}{(R^2 + \rho^2 - 2R\rho\cos\phi)^{1/2}} \right\} \Delta\rho \tag{23a}$$

$$+\frac{1}{r_2}\left(\cos\phi\ \frac{\rho}{r_2}\sin\phi-\sin\phi\ \sqrt{1-\frac{\rho^2}{r_2^2}\sin^2\phi}\right)\Delta\dot{\rho} \tag{23b}$$

$$+\frac{1}{r_2}\Bigg\{(\rho\cos\phi\,\dot{\phi}-\dot{\rho}\sin\phi)\ \frac{\rho}{r_2}\sin\phi$$

$$+(R\,\omega\sin\omega t+\rho\sin\phi\,\dot{\phi}+\dot{\rho}\cos\phi)\left(\frac{\rho\cos\phi}{r_2}-\frac{\rho\sin\phi}{r_2^3}R\rho\sin\phi\right)$$

$$-(\rho\sin\phi\,\dot{\phi}+\dot{\rho}\cos\phi)\ \sqrt{1-\frac{\rho^2}{r_2^2}\sin^2\phi}+(R\,\omega\cos\omega t+\rho\cos\phi\,\dot{\phi}-\dot{\rho}\sin\phi)$$

$$\times\left(-\frac{2\rho^2\sin\phi\cos\phi}{r_2^2}+\frac{2\rho^2\sin^3\phi\,R\rho}{r_2^4}\right)$$

$$-\frac{1}{r_2}\Bigg[(R\,\omega\sin\omega t+\rho\sin\phi\,\dot{\phi}+\dot{\rho}\cos\phi)\ \frac{\rho}{r_2}\sin\phi$$

$$+(R\,\omega\cos\omega t+\rho\cos\phi\,\dot{\phi}-\dot{\rho}\sin\phi)\ \sqrt{1-\frac{\rho^2}{r_2^2}\sin^2\phi}\Bigg]$$

$$\times\frac{R\rho\sin\phi}{(R^2+\rho^2-2R\rho\cos\phi)^{1/2}}\Bigg\}\ \Delta\phi \tag{23c}$$

$$+\frac{1}{r_2}\left(\rho\sin^2\phi\,\frac{\rho}{r_2}+\rho\cos\phi\ \sqrt{1-\frac{\rho^2}{r_2^2}\sin^2\phi}\right)\Delta\dot{\phi} \tag{23d}$$

$$+\frac{1}{r_2}\Bigg\{\omega \sin \omega t \frac{\rho}{r_2} \sin\phi - (R\,\omega \sin \omega t + \rho \sin\phi\,\dot{\phi} + \dot{\rho} \cos\phi)\frac{\rho \sin\phi}{r_2^3}(R - \rho\cos\phi)$$

$$+ \omega \cos \omega t \sqrt{1 - \frac{\rho^2}{r_2^2}\sin^2\phi} + (R\,\omega \cos \omega t + \rho \cos\phi\,\dot{\phi} - \dot{\rho} \sin\phi)$$

$$\left(1 - \frac{\rho^2}{r_2^2}\sin^2\phi\right)^{-1/2} \times \frac{\rho^2 \sin^2\phi}{r_2^4}(R - \rho\cos\phi)$$

$$-\frac{1}{r_2}\Bigg[(R\,\omega \sin \omega t + \rho \sin\phi\,\dot{\phi} + \dot{\rho} \cos\phi)\frac{\rho}{r_2}\sin\phi$$

$$+ (R\,\omega \cos \omega t + \rho \cos\phi\,\dot{\phi} - \dot{\rho} \sin\phi)\sqrt{1 - \frac{\rho^2}{r^2}\sin^2\phi}\Bigg]$$

$$\times \frac{R - \rho\cos\phi}{(R^2 + \rho^2 - 2R\rho\cos\phi)^{1/2}}\Bigg\}\Delta R \qquad (23e)$$

$$+\frac{1}{r_2}\Bigg[(R \sin \omega t + \omega^2 R \cos \omega t)\frac{\rho}{r_2}\sin\phi$$

$$+ (R \cos \omega t - \omega^2 R \sin \omega t)\sqrt{1 - \frac{\rho^2}{r_2^2}\sin^2\phi}\Bigg]\Delta\omega \quad . \qquad (23f)$$

7. CORRECTIONS TO IDEALIZED MODELS

The redshift equation, equation (1), and the various other forms derived in the preceding study (Jaffe and Vessot, 1973) are completely general; they have been set up without any restrictions on β_i. Our idealized model here has assumed a "point" earth moving in a perfect circle around the sun; the velocity of revolution is ~30 km/sec. Of course, the earth is not a point, and it is necessary to investigate what corrections to our present analysis would be introduced by considering a more realistic model of the earth.

The earth has a mean radius of ~6400 km and rotates on its axis with a velocity of rotation of ~0.47 km/sec. Since this velocity of rotation is about two orders of magnitude less than the velocity of revolution around the sun, it is not necessary to include the secondary velocity effects in this present determination of the greatest permissible uncertainty in the tracking parameters. Similarly, since the earth's radius is approximately four orders of magnitude less than the earth–sun distance, inclusion of a finite-radius earth in the transformation to a geodetic system would negligibly change the resultant equations here.

All secondary effects, such as the earth's rotation, motion about the earth–moon barycenter, and the earth and moon's actual gravitational potential, can be included in the final working program, by use of the completely general formalism already derived. As was emphasized in the preceding study (Jaffe and Vessot, 1973), all coordinates, parameters, and constants must eventually be written in an operational framework, completely in terms of observables (invariants), in order to eliminate any ambiguity in the interpretation of a coordinate system.

8. ANALYSIS OF TRACKING-ACCURACY REQUIREMENTS FOR HELIOCENTRIC PROBE MODEL ORBITS

The perturbation equations derived in the preceding sections were programed and applied to various model orbits of a heliocentric probe, such as the proposed NASA–ESRO heliocentric satellite mission.

The general analysis of the tracking-accuracy requirements is as follows: For a given time in the orbit, all the various-order terms in the redshift were calculated. The smallest term was then used to determine the maximum allowable uncertainties in the heliocentric parameters, as given by the equations in Section 4. These uncertainties in the heliocentric parameters were then converted to corresponding uncertainties in the geodetic parameters, through the equations in Sections 5 and 6. Obviously, an uncertainty in a geodetic parameter such as ρ could correspond to uncertainties in more than one heliocentric parameter, in this case, r_2, θ_2, β_{r_2}, β_{θ_2}; all these possibilities were computed, commensurate with the actual allowable uncertainties in the heliocentric parameters, and the program then chose the maximum uncertainty in each case. The results are shown in Figures 2 to 4.

9. STATE OF THE ART IN DEEP-SPACE-PROBE TRACKING

The present state of the art in deep-space-probe tracking is illustrated in Table 1, which gives the 1-sigma accuracies achievable with observations carried out both with present-day and with projected future capabilities in instrumentation and data-processing methods. The given values do not take into account the possible contributions to the achievable maximum accuracy coming from a priori knowledge of the space trajectory.

All figures apply to dual-frequency observations, which remove the effects of the interplanetary plasma as well as those of the earth's ionosphere. The angular accuracy values apply to earth-based very long-baseline interferometry (VLBI) systems, in which tropospheric effects have been removed (down to 0.1%) by columnar radiometric observations (conducted at water vapor and oxygen absorption lines) of the tropospheric path along the direction of, and simultaneously with, the VLBI beam. The angular accuracy figures could be substantially lowered (to 10^{-9} or even 10^{-10} rad) by using a 100,000-km VLBI baseline established between two satellites, thereby totally removing the effect of the time-variable and space-variable earth's atmosphere. With this spaceborne VLBI system, the angular rate accuracies could be improved to 10^{-13} or 10^{-14} rad/sec.

Table 1. Achievable Accuracies with State-of-the-Art Deep-Space-Probe Tracking Techniques

Capability	Radial range (m)	Radial velocity (mm/sec)	Angle (rad)	Angular velocity (rad/sec)
Present	16	0.5	2×10^{-7}	10^{-12}
Future	1	0.05	2×10^{-8}	10^{-13}

10. COMPARISON OF REQUIRED AND CURRENTLY ACHIEVABLE TRACKING ACCURACY

The analysis indicates that the current tracking capability is sufficient to determine the range ρ and earth–sun distance R accurately enough for a second-order redshift experiment. The JPL Deep Space Network (DSN) tracking program, for example, has a present range tracking accuracy of approximately 16 m and a projected, future accuracy of about 1 m.

With regard to range rate $\dot{\rho}$, for all model orbits considered, the present conventional tracking schemes are about two orders of magnitude too crude for some parts of the probe orbit, but nearly sufficient near perihelion (which corresponds to the greatest possible redshift with respect to the earth). The projected, future accuracy is still a bit less than is required over the entire orbit.

The angular tracking accuracy ϕ is also too crude in the regions far from perihelion by roughly three orders of magnitude. Proposed accuracy for earth-based terminals is still roughly two orders of magnitude too crude in these regions, even with the assumption of the best estimate for earth-based VLBI tracking in the near future. As mentioned in Section 9, a VLBI tracking system using satellites in earth orbit, although a somewhat distant possibility, would be one way, for example, to achieve the required tracking accuracy.

The angular velocity $\dot{\phi}$ and ω requirements are quite stringent for all model orbits. This question requires more detailed study and depends on the specific tracking scheme to be used.

11. CLOCK ACCURACY REQUIREMENTS

We can determine the necessary performance required of the clocks for a test of the second-order redshift term by plotting the minimum β^4 term in the redshift as a function of the orbital time. Figures 5 to 7 indicate that the requirements are least stringent near perihelion, where the redshift is maximal. (The curves are, of course, not necessarily symmetric around perihelion, since the relative juxtaposition of the probe and earth at different times will cause the β^4 or $m\beta^2$ terms to become as significant as the pure m^2 term.)

The present state of the art in atomic clocks is advancing toward stability in the 10^{-16} region, for averaging intervals of the order of 10^5 to 10^6 sec. Ground-based maser devices have already shown stability of 2 parts in 10^{15} for time intervals of 10^3 to 10^4 sec. Development is in progress of a space-qualified hydrogen-maser clock for a terrestrial probe experiment; development of space-qualified cesium and rubidium devices is also expected in the next few years.

12. RECOMMENDATIONS

This perturbation analysis is intended to present the "worst case" situation. It has maximized the tracking requirements for the second-order redshift experiment. Correlations of the parameters with respect to the earth and probe orbits, which would probably tend to make the actual requirements somewhat less stringent, have still to be considered. This further study requires more extensive effort and is recommended as the next step in the analysis of a second-order redshift experiment.

13. REFERENCES

Jaffe, J., 1969. Collapsing objects and the backward emission of light. Ann. Phys., vol. 55, p. 374.

Jaffe, J., and Vessot, R. F. C., 1973. The second-order gravitational redshift. Final Report for Phase I of NASA Research Grant NGR 09-015-205.

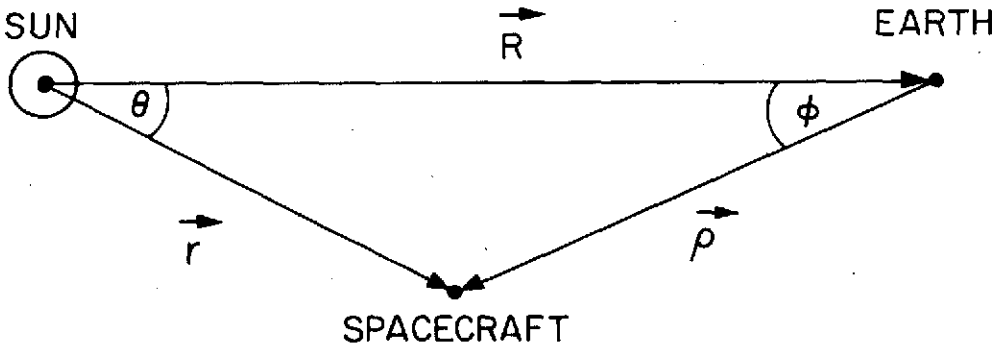

Figure 1. Tracking geometry.

Figures 2, 3, and 4. Allowable uncertainties in the geodetic parameters, as a function of the probe period. A plot of the earth–sun distance uncertainty ΔR, and the earth's angular velocity of revolution $\Delta\omega$, have been omitted for simplicity; they are either of the same order, or approximately 50% more stringent, than $\Delta\rho$ and $\Delta\dot{\phi}$, respectively.

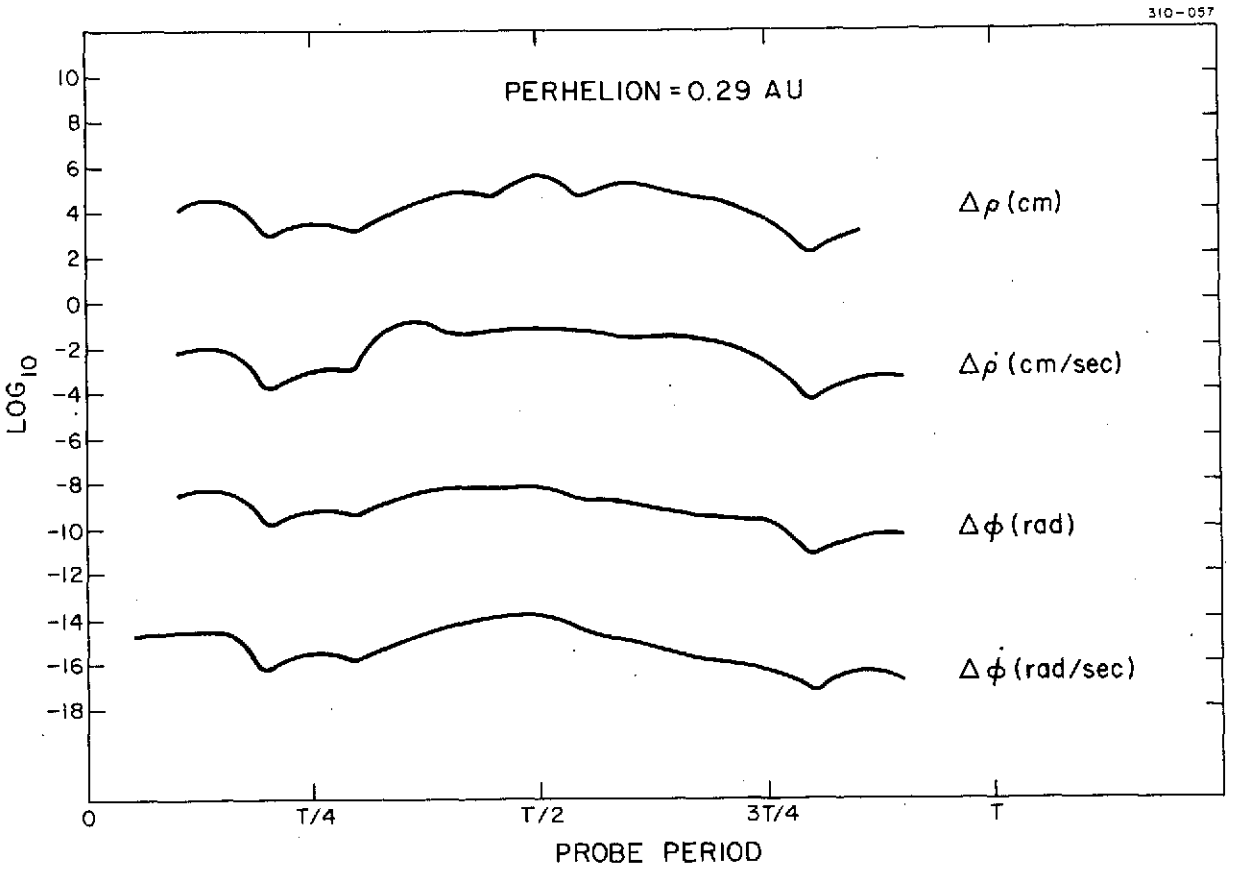
310-057
PERHELION = 0.29 AU
10
8
6
4
2
0
-2
-4
-6
-8
-10
-12
-14
-16
-18
LOG10
Δρ (cm)
Δρ̇ (cm/sec)
Δφ (rad)
Δφ̇ (rad/sec)
0
T/4
T/2
3T/4
T
PROBE PERIOD

Figure 2.

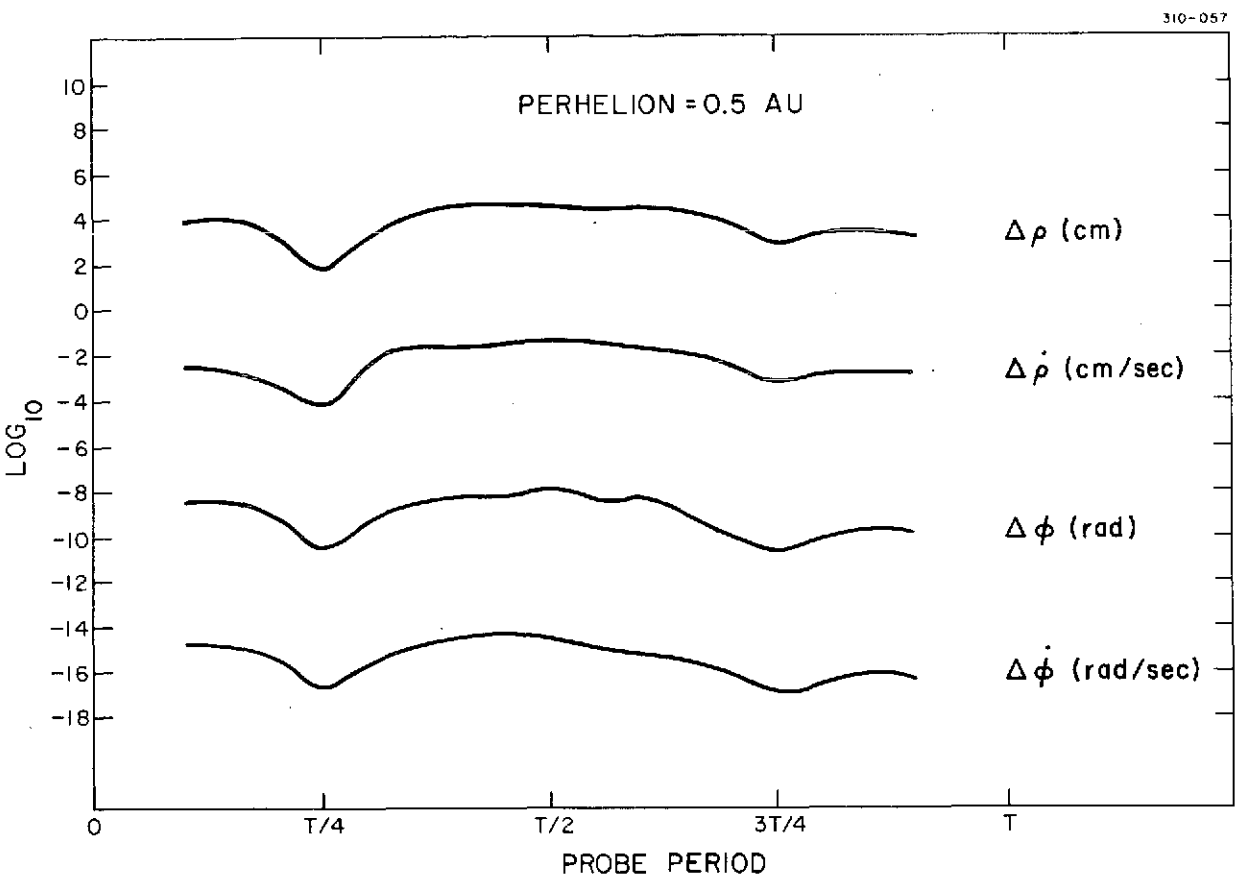
310-057
PERHELION = 0.5 AU
10
8
6
4
2
0
-2
-4
-6
-8
-10
-12
-14
-16
-18
LOG10
Δρ (cm)
Δρ̇ (cm/sec)
Δφ (rad)
Δφ̇ (rad/sec)
0
T/4
T/2
3T/4
T
PROBE PERIOD

Figure 3.

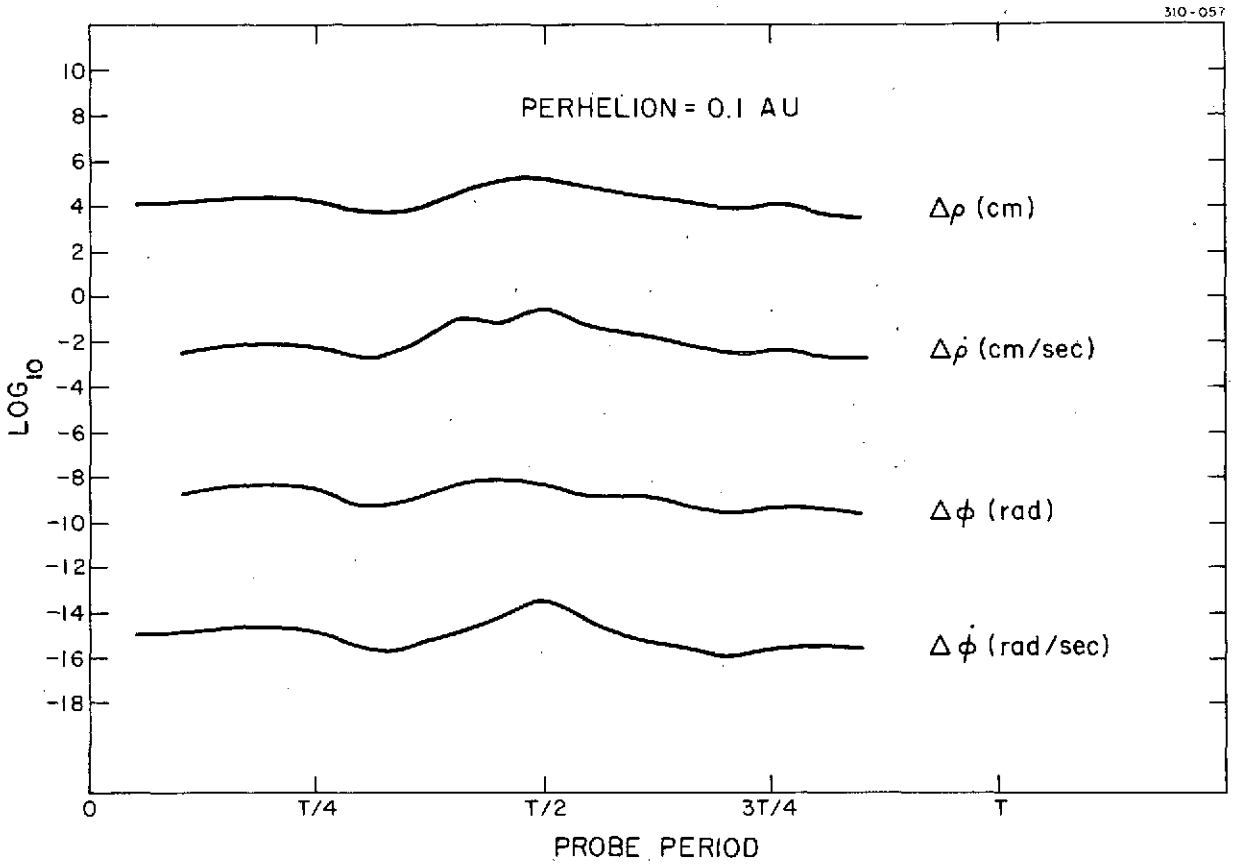
310-057
PERHELION = 0.1 AU
$\Delta\rho$ (cm)
$\Delta\dot{\rho}$ (cm/sec)
$\Delta\phi$ (rad)
$\Delta\dot{\phi}$ (rad/sec)
LOG$_{10}$
10
8
6
4
2
0
-2
-4
-6
-8
-10
-12
-14
-16
-18
0
T/4
T/2
3T/4
T
PROBE PERIOD

Figure 4.

Figures 5, 6, and 7. Minimum term of order c^{-4}, as given by equation (1), as a function of probe period.

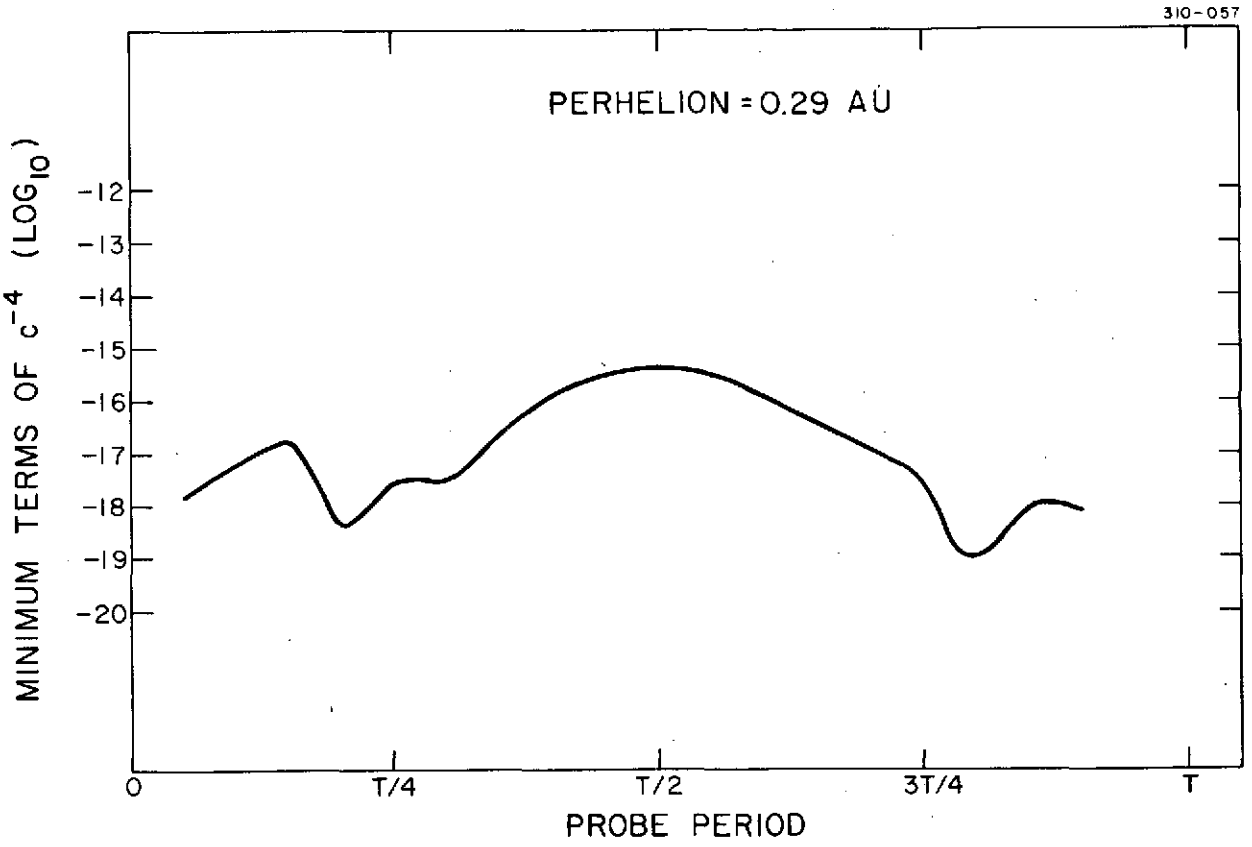
310-057
PERHELION = 0.29 AU
MINIMUM TERMS OF c^{-4} (LOG_{10})
-12
-13
-14
-15
-16
-17
-18
-19
-20
0
T/4
T/2
3T/4
T
PROBE PERIOD

Figure 5.

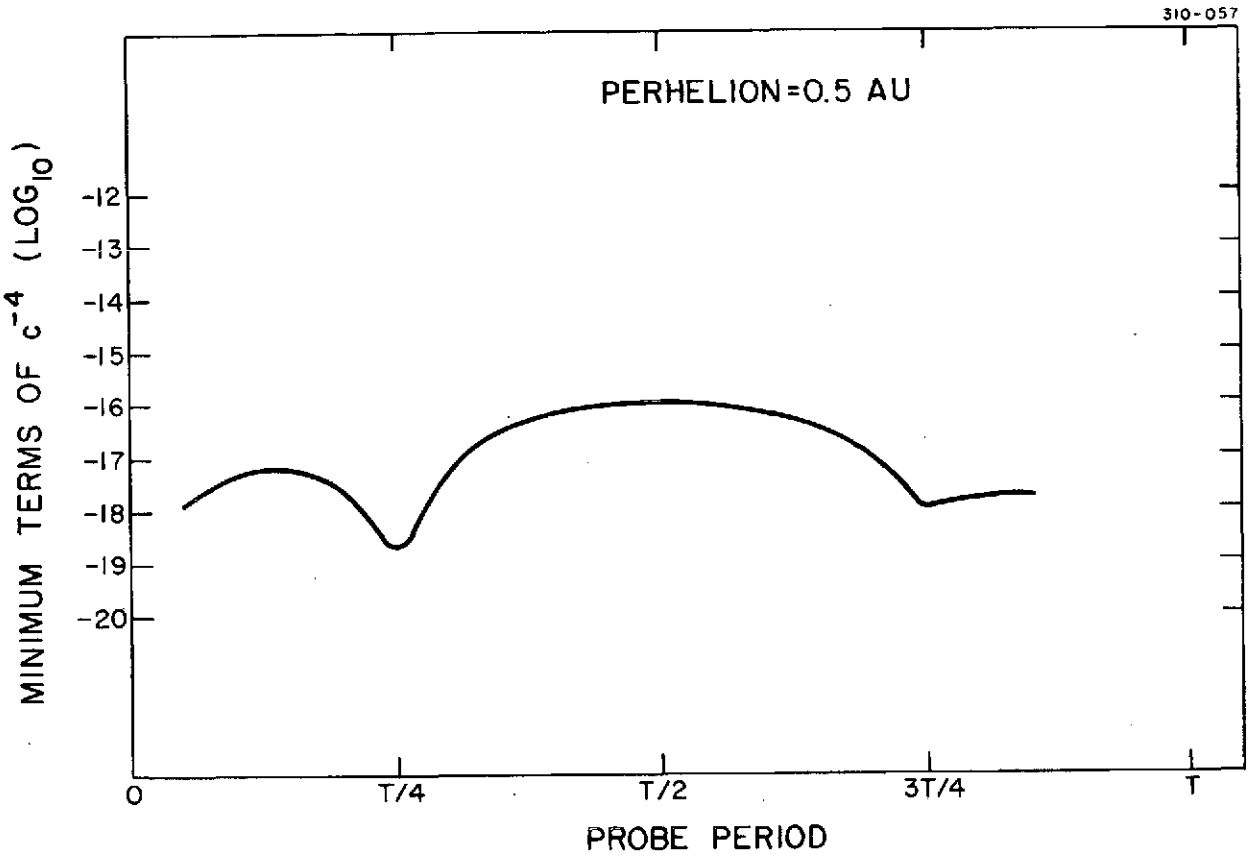
310-057
PERHELION=0.5 AU
MINIMUM TERMS OF c^{-4} (LOG_{10})
-12
-13
-14
-15
-16
-17
-18
-19
-20
0
T/4
T/2
3T/4
T
PROBE PERIOD

Figure 6.

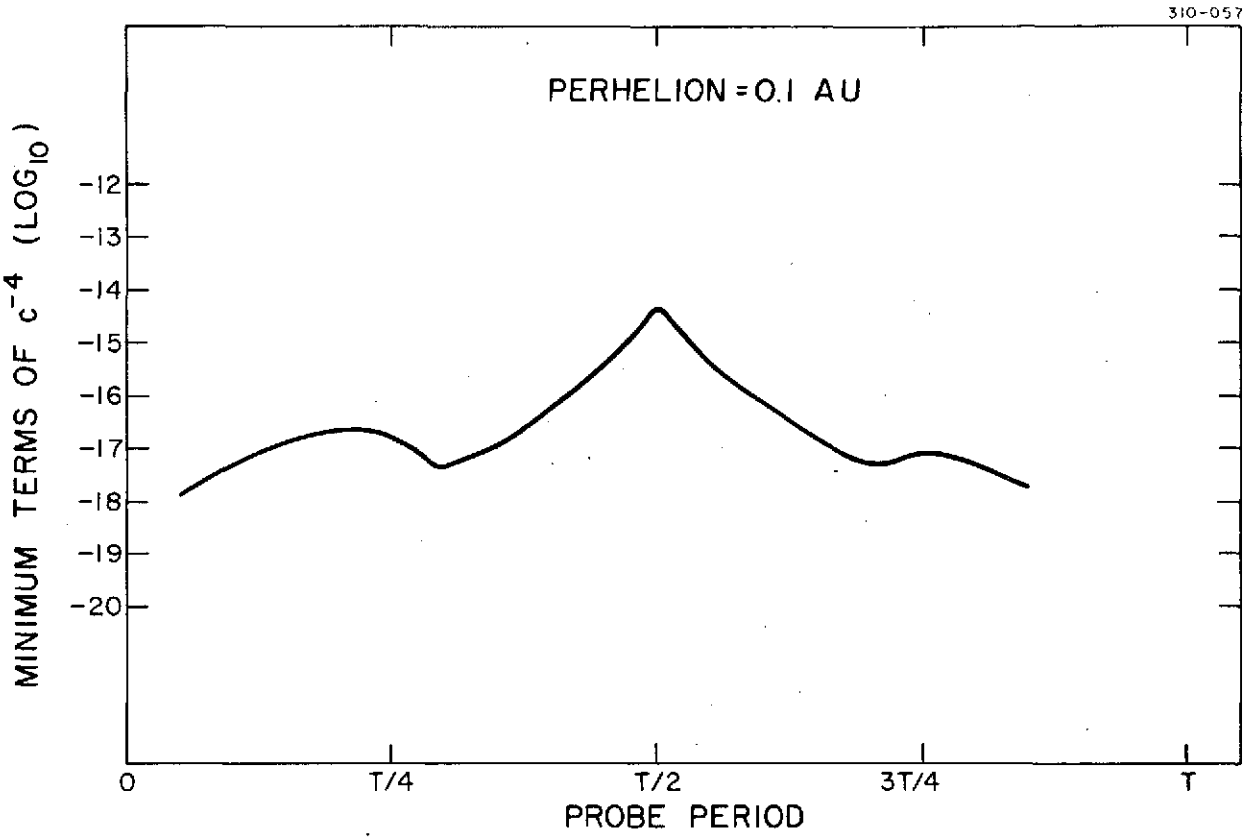
310-057
PERHELION = 0.1 AU
MINIMUM TERMS OF c^{-4} (LOG_{10})
-12
-13
-14
-15
-16
-17
-18
-19
-20
0
T/4
T/2
3T/4
T
PROBE PERIOD

Figure 7.